Postglacial evolution of a Pacific coastal fjord in British Columbia, Canada: interactions of sea-level change, crustal response, and environmental fluctuations — results from MONA core MD02-2494[1]

Audrey Dallimore, Randolph J. Enkin, Reinhard Pienitz, John R. Southon, Judith Baker, Cynthia A. Wright, Tom F. Pedersen, Steve E. Calvert, Tara Ivanochko, and Richard E. Thomson

Abstract: The sedimentary record in a 40.9 m giant (Calypso) piston core (MD02-2494) raised from the inner basin within Effingham Inlet, British Columbia, Canada, during the 2002 Marges Ouest Nord Américaines (MONA) campaign, spans from 14 360 ^{14}C years BP (17 300 calibrated calendar (cal.) years BP) to about nine centuries before present. The core archives changes in sedimentation and sea level immediately following deglaciation of the Late Wisconsin Fraser Glaciation, which peaked about 15 000 ^{14}C years BP. The presence of the Mazama Ash in the core anchors a detailed chronology based on 49 radiocarbon dates and seven Pleistocene paleomagnetic secular variation correlations. Diatom assemblages identify a marine–freshwater–marine transition in the basin, which occurred 11 630 ^{14}C years BP (13 500 cal. years BP). At this time, a bedrock sill, presently at 46 m depth, was briefly exposed as sea level fell and then rose again during isostatic crustal adjustments. These data constrain a new sea-level curve for the outer coast of Vancouver Island covering the past 12 000 ^{14}C years BP (14 000 cal. years BP), providing new information on the nature of deglaciation along the west coast of Canada and informing interpretations of regional paleoceanographic records and mantle viscosity models.

Résumé : Les données sédimentaires enregistrées dans une carotte (MD02-2494) de 40,9 m prélevée par un carottier géant à piston (Calypso) dans le bassin interne du passage Effingham, Colombie-Britannique, Canada, au cours de la campagne MONA (Marges Ouest Nord-Américaines) couvrent une période allant de 14 360 années ^{14}C avant le présent (17 300 années calendaires avant le présent – années cal. BP) à environ neuf siècles avant le présent. La carotte enregistre les changements dans la sédimentation et les niveaux de la mer immédiatement après la déglaciation de la glaciation de la fin du Wisconsinien (Fraser) dont la crête a eu lieu vers 15 000 années ^{14}C BP. La présence de cendre volcanique Mazama dans la carotte confirme une chronologie détaillée basée sur 49 datations au radiocarbone et 7 corrélations paléomagnétiques de variations séculaires datant du Pléistocène. Les assemblages de diatomées identifient une transition marine-eau douce-marine dans le bassin à 11 630 années ^{14}C BP (13 500 années cal. BP). À cette époque, un filon couche du socle, maintenant à une profondeur de 46 m, a été brièvement exposé alors que le niveau de la mer a chuté et ensuite remonté durant les ajustements isostatiques de la croûte. Ces données imposent des limites à une nouvelle courbe de niveau de la mer pour la côte Ouest de l'île de Vancouver pour les dernières 12 000 ^{14}C années avant le présent (14 000 années cal. BP); elles fournissent de nouvelles informations quant à la nature de la déglaciation le long de la côte Ouest du Canada et contribuent à orienter les interprétations des données paléocéaniques régionales et les modèles de viscosité du manteau.

[Traduit par la Rédaction]

Received 15 March 2008. Accepted 25 August 2008. Published on the NRC Research Press Web site at cjes.nrc.ca on 5 November 2008.

Paper handled by Associate Editor P. Hollings.

A. Dallimore.[2] School of Environment and Sustainability, Royal Roads University, 2005 Sooke Road, Victoria, BC V9B 5Y2, Canada.
R.J. Enkin and J. Baker. Geological Survey of Canada-Pacific, Institute of Ocean Sciences, Sidney, BC V8L 4B2, Canada.
R. Pienitz. Département de Géographie & Centre d'études nordiques, Université Laval QC, QC G1V 0A6, Canada.
J.R. Southon. Department of Earth System Science, University of California, Irvine, CA 92697-3100, USA.
C.A. Wright and R.E. Thomson. Department of Fisheries and Oceans, Institute of Ocean Sciences, 9860 West Saanich Road, Sidney, BC V8L 4B2, Canada.
T.F. Pedersen. School of Earth and Ocean Sciences, University of Victoria, P.O. Box 3055, Stn. CSC, Victoria, BC V8W 2Y2, Canada.
S.E. Calvert and T. Ivanochko. Earth and Ocean Sciences, University of British Columbia, 6339 Stores Rd, Vancouver, BC V6T 1Z4, Canada.

[1]This article is one of a series of papers published in this Special Issue on the theme *Polar Climate Stability Network*.
[2]Corresponding author (e-mail: Audrey.dallimore@royalroads.ca).

 doi:10.1139/E08-042

Introduction

The new 40.9 m long, Effingham Inlet core described in this paper is to date the best high-resolution Holocene sediment record for the northeastern Pacific Ocean and extends the known record of environmental and tectonic conditions in the area back ∼14 ^{14}C millennia to earliest deglacial times following the recession of the continental Fraser Glaciation (Clague 1989). The core was raised as part of the 2002 Marges Ouest Nord Américaines (MONA) campaign, which was a multinational cruise of the International Marine Global Changes Program (Beaufort 2002). A new paleosea-level curve presented in this paper identifies the timing of postglacial crustal stabilization, providing the framework for a high-resolution paleoenvironmental statistical analyses using data from geochemical and physical properties of the core sediments (Ivanochko et al. 2008). This paper also interprets the paleoenvironmental conditions of the west coast of Vancouver Island for the entire Holocene, which include profound and rapid changes in sea level and coastal ocean dynamics as glaciers receded from the west coast of Canada. The collective work on the core provides millennia of high-resolution north Pacific paleoceanographic and paleoenvironmental data that can be directly compared with the north Pacific paleoatmospheric data from the Mount Logan ice core (Osterberg et al. 2008). These two records contribute to our understanding of the north Pacific climate system and forcing mechanisms (Fisher et al. 2003; Wake et al. 2006).

An understanding of postglacial sedimentation and sea-level changes is also of interest to shore-zone engineers and planners involved in future coastal and offshore development (Barrie and Conway 2002*a*, 2002*b*), as well as ecologists and archaeologists with interests in coastal fisheries, ecosystems, and cultures (Josenhans et al. 1995, 1997; Fedje and Josenhans 2000; Hetherington et al. 2003; McKechnie 2005). Precise relative sea-level curves also give valuable information for geophysical modelling of crustal response and mantle rheology in this seismically active area, since geodetic observations measuring crustal strain leading to earthquakes must be corrected for isostatic adjustments of the crust (Wang et al. 2001; James et al. 2005).

Regional setting

Effingham Inlet is a 17 km long multiple-silled marine fjord, which is connected to the Pacific Ocean through Barkley Sound, on the southwestern coast of Vancouver Island, British Columbia (B.C.) (Fig. 1). The fjord is rimmed by steep bedrock walls and has an inner basin (120 m depth) and an outer basin (205 m depth); each basin is isolated from the open ocean waters by shallow bedrock sills. Consequently, the bottom waters of the inner basin are usually anoxic (Patterson et al. 2000; Dallimore et al. 2005*a*). Water property distributions in the modern inlet are characteristic of a weakly mixed estuary (Thomson 1981) with small (<2 m) tidal variation and negligible bottom currents.

Cores covering the late Holocene in Effingham Inlet contain annually laminated sediments that are rare and valuable high-resolution (annual) archives, offering the opportunity to link past records of terrestrial climate and environmental change with offshore oceanographic conditions on a number of time scales (Kennett and Ingram 1995; Pike and Kemp 1996*a*; Sancetta 1996; Kemp 1996, 2003; Ware and Thomson 2000; Dallimore et al. 2005*a*, 2005*b*). The variability in preservation and deposition of the annual winter laminae, which record variation in precipitation, and the spring to summer diatomaceous laminae, which are indicative of annual productivity in the coastal ocean, archive the abrupt crossing of depositional thresholds that are related to climate changes (Dallimore 2001; Chang et al. 2003; Hay et al. 2003; Dallimore et al. 2005*a*, 2005*b*; Hay et al. 2007).

Similarly, the occurrence of unlaminated mud units (homogenites) intercalated amongst the laminated sediments can be interpreted in terms of climatically related wind-induced disruptions of the coastal ocean dynamics (Dallimore et al. 2005*a*). Other unlaminated sedimentary units in the core are interpreted to be associated with seismic shaking and (or) sediment slumping (seismites and debris flows), and these may testify to large earthquake events at the northern Cascadia subduction zone along the tectonically active B.C. coast (Clague et al. 1982; Rogers 1988; Hyndman 1995; Goldfinger et al. 2003*a*, 2003*b*; Dallimore et al. 2005*a*, 2005*b*).

Glacial and sea-level history of the west coast of Canada

The Cordilleran ice sheet covered British Columbia, the southern part of Yukon Territory, and southern Alaska during the Fraser Glaciation (ca. 30 000 – 11 000 years BP). At the glacial maximum (ca. 15 000 ^{14}C years BP, 18 000 cal. years BP), the ice sheet was up to 2000 m thick and extended to the shelf edge off the west coast of Vancouver Island (Clague 1983, 1989, 1994; Luternauer et al. 1989*a*, 1989*b*; James et al. 2000; Clague and James 2002). Ice retreat progressed sequentially along the BC coast from north to south, beginning first in the Queen Charlotte Basin to the north (Fig. 1) ca. 16 000 ^{14}C years BP (∼18 500 cal. years BP). Ice disappeared from the west coast ca. 14 000 ^{14}C years BP (16 750 cal. years BP; Ward et al. 2003) and then from the east coast of the island and the Georgia Basin (Fig. 1) after 12 400 ^{14}C years BP (14 250 cal. years BP; Clague 1989, 1994; Barrie and Conway 1999, 2002*b*). By ∼10 000 ^{14}C years BP, ice cover in British Columbia had about the same areal extent as today (Clague and James 2002).

Rapid changes in sea level of up to 200 m over several centuries occurred on the BC coast immediately following deglaciation, caused by a complex interaction between glacio-isostatic crustal adjustments and changes in eustatic sea level throughout the Late Pleistocene and Holocene, and further complicated by tectonic activity along the Cascadia subduction zone (Fig. 1; Clague 1994). Only cursory information on sea level in immediate postglacial time is available for the west coast of Vancouver Island. Sea level fell from ∼50 to 100 m above present datum immediately following deglaciation to below present datum in the early Holocene (Clague 1981, 1994; Clague et al. 1982; Clague and James 2002; Mosher and Hewitt 2004). Sea level rose to about +4 m at 5500 ^{14}C years BP and has since fallen to present levels (Mathews et al. 1970; Hebda and Rouse 1979; Howes 1981; Clague 1981, 1994; Clague et al. 1982; Hutchinson 1992; Friele and Hutchinson 1993; Clague and James 2002). No data exists, however, to constrain the precise timing or position of the early Holocene lowstand.

Fig. 1. (A) Location of Effingham Inlet, the regional geography, and the tectonic setting. (B) Core site and the central thalweg of the inlet, which is illustrated in cross section in (C).

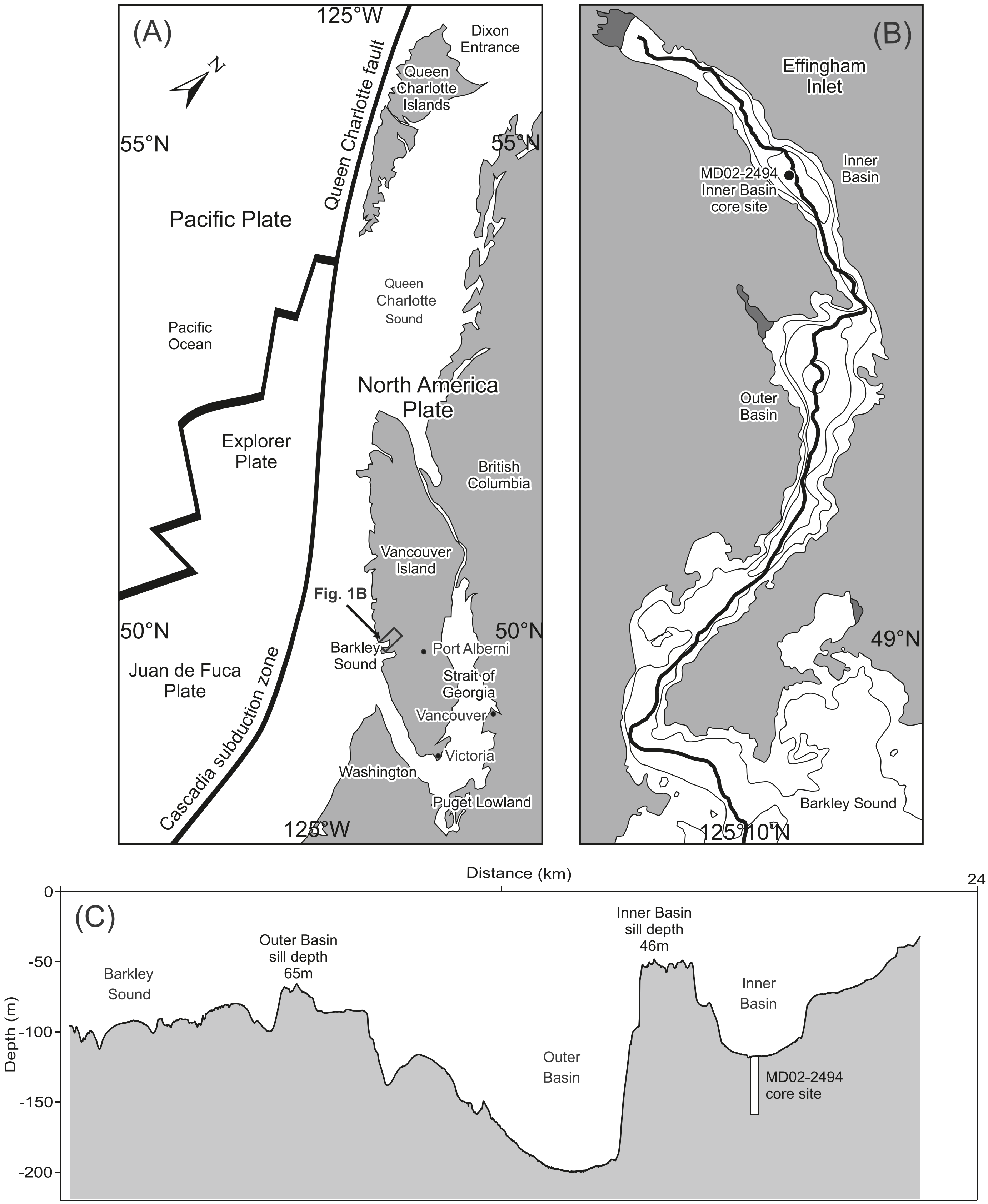

Fig. 2. Multibeam imagery of Effingham Inlet. A meandering paleochannel, presently at 46 m depth is evident between the inner and outer basins.

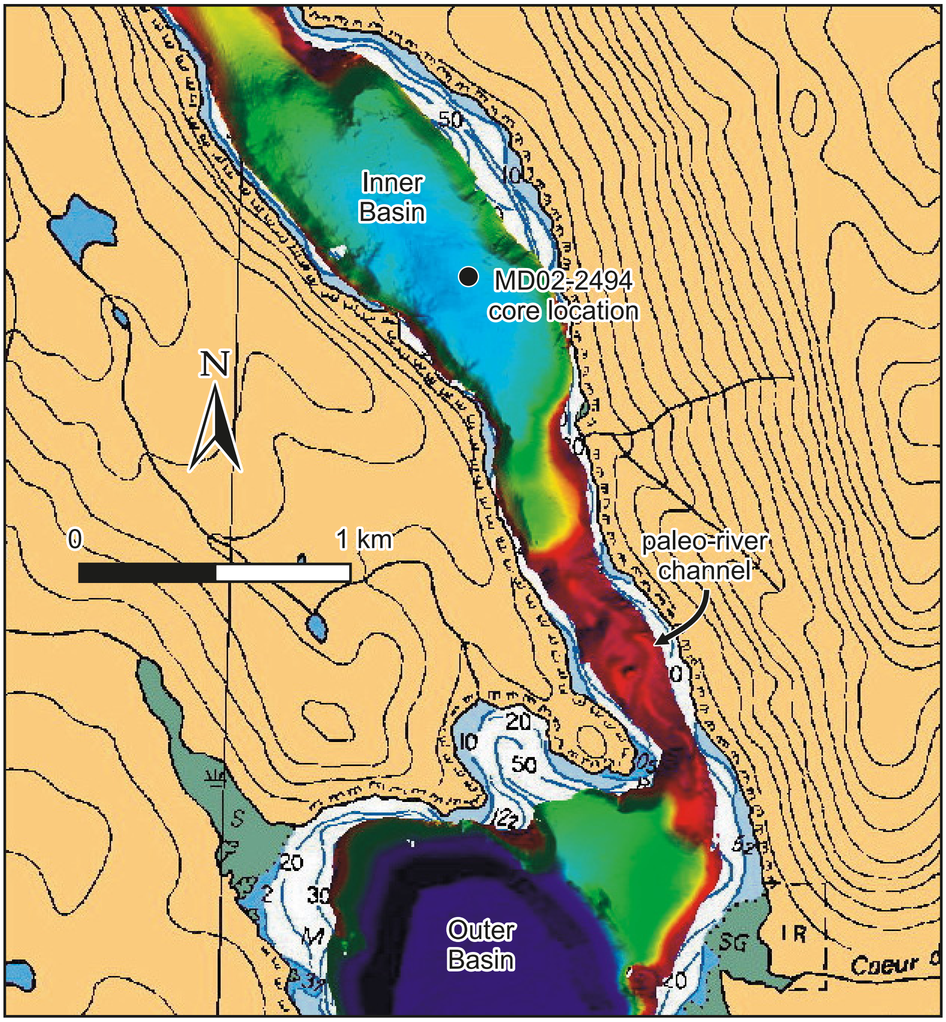

More is known about the sea-level history to the east in Georgia Basin where relative sea level was 80–100 m higher than today during a sea-level transgression as deglaciation progressed (Barrie and Conway 2002*b*; James et al. 2005). In contrast, the outer coast of Vancouver Island was tilted up towards the mainland during deglaciation with an accompanying sea-level regression at ~12 500 ^{14}C years BP (14 250 cal. years BP). In other words, a sea-level regression was occurring in Effingham Inlet contemporaneously with a sea-level transgression in the Strait of Georgia and these are probably linked, perhaps because of lateral movement of material in the asthenosphere (Hetherington and Barrie 2004).

Materials and methods

Bathymetric imaging

Multibeam bathymetric data for Effingham Inlet (Fig. 2) were collected in April 2005 aboard the Canadian Coast Guard Ship (CCGS) *Vector* using Kongsberg–Simrad's EM-3000 multibeam echo sounder, which operates at a frequency of 300 kHz utilizing 127 beams with survey speeds averaging 6 kn. A differential global positioning system was used for navigation, providing a horizontal positional accuracy of ±3 m. The sound velocity of the ocean was measured periodically during the survey and used to correct the effect of sonar beam refraction and data were adjusted for tidal variation using tidal predictions from the Canadian Hydrographic Service.

Sedimentology

A 40.9 m long sediment core (MD02-2494) was raised using the Calypso piston core system on-board the French ship the *RV Marion Dufresne*, in the inner basin of Effingham Inlet (49°04.28′N, 125°09.55′W, water depth 120 m) in June 2002 (Fig. 1; Beaufort 2002). The recovered core length is 40.32 m with an additional 60 cm extruded from the liner when the core was opened (total recovered length, 40.9 m). The core was visually logged on-board ship and color reflectance was measured using a Minolta 2022 spectrophometer (Beaufort 2002). Subsequently, detailed analyses of the lithology were carried out in the laboratories of the Geological Survey of Canada Pacific (GSC Pacific), housed at the Institute of Ocean Sciences, Sidney, British Columbia. Sediment slabs (20 cm long, 4 cm wide, and 1 cm thick) of the entire core from the center of one core half were X-rayed using conventional medical X-radiography equipment and Kodak min-R 2000 single screen mammography film (Pike and Kemp 1996*b*; Axelsson 2002; Dallimore et al. 2005*a*) to enable observation of the fine sedimentological details. Detailed photographs, X-radiographs, and core logs can be found in Dallimore et al. 2008.

Physical properties

Magnetic properties of the core were measured at the Paleomagnetism Laboratory at GSC Pacific on discrete samples oriented with respect to the core. Cylindrical subsamples (2.5 cm diameter, 2.2 cm long plastic vials) were removed from the split core every 10 cm. Magnetic remanence was measured with an Agico JR5-A spinner magnetometer. Unstable magnetism was cleaned using a Schonstedt GSD-5 with tumbler for alternating field demagnetization. Peak fields up to 100 mT were applied on pilot samples, but three demagnetization steps up to 20 mT were found sufficient for most samples. Magnetic mineralogy was estimated to establish proxy measurements for sediment provenance using a Sapphire SI2B susceptibility meter and a J meter coercivity spectrometer (cf. Enkin et al. 2007).

Geochronology and age model

Radiocarbon dating

A total of 49 samples of wood and plant (34 samples) and shell (15 samples) material were recovered from the core at GSC Pacific for accelerator mass spectrometry (AMS) radiocarbon dating performed at the Keck Carbon Cycle AMS Program, University of California, Irvine, California. Care was taken in sampling to avoid homogenite, debris flow, and seismite units that represent reworking of sediment (Dallimore et al. 2005*a*). Results are reported in radiocarbon years BP (^{14}C years BP) and also as calibrated calendar years (cal. years BP), rounded to the nearest decade, which were calculated using the CALIB version 5 program and the INTCAL04 database for terrestrial (wood) material, relative to 1950 AD. The reservoir correction used for marine shell material (ΔR = 330 ± 90 years, Holocene; ΔR = 810 ± 130 years, Pleistocene) is based on the MARINE98 database for this area (Robinson and Thompson 1981; Southon et al. 1990; Stuiver and Reimer 1986, 1993; Stuiver and Braziunas 1993; Stuiver et al. 1998*a*, 1998*b*; Hutchinson et al. 2004*b*). Two small pieces of wood (University of California, Irvine, accelerator mass spectrometry (UCIAMS) 2288, 2289) were sampled from 2161 cm, giving a contemporaneous pair. Nine samples of shell material (UCIAMS 2296–2304) from a 3 cm interval from 3158 to 3161 cm were sampled to compare shell error ranges.

Tephra analyses

Four potential tephra samples (from 1342, 1646, 2346, and 2356 cm), which were identified visually in core sample and on X-radiograph negatives as thin (mm scale), very bright units, were examined optically at the Department of Geology, University of Toronto, Toronto, Ontario, and by electron microprobe analysis (sample from 1646 cm) using a 6 μ wide beam.

Paleosecular variation age analyses

Magnetic declination and inclination records were used to supplement the radiocarbon data from the bottom 7 m of the core that contained little or no organic material. Dating sediment sequences by magnetic secular variation is accomplished by correlating swings, peaks, and valleys in the magnetic declination and inclination records to reference curves established from well-dated sequences from Mono Lake, California (Lund et al. 1988).

Micropaleontology

Diatom analyses on 43 sediment samples from representative glacial and immediately postglacial lithofacies units in the lower half of the core were carried out at the Paleolimnology–Paleoecology Laboratory at Université Laval, Québec City, Quebec. The sediment subsamples were digested with 30% hydrogen peroxide (H_2O_2) in a hot water bath. Digested samples with siliceous material were then repeatedly centrifuged and decanted with distilled water to remove acids. Coarse sand was removed by decanting. For samples with high proportions of clay-sized material, heavy-liquid separation using sodium polytungstate was used to concentrate diatom valves. An aliquot of the prepared slurry was settled onto cover slips and evaporated over a 24 h period. Once dry, the cover slips were mounted onto microscope slides in Naphrax permanent diatom mountant with a high refractive index (RI = 1.71). Diatom identifications were made to the lowest taxonomic level possible using a Leica DMRB microscope at magnifications between 400× and 1000×, with reference to publications on diatom floras from coastal regions (Campeau et al. 1999; Witkowski et al. 2000; Pienitz et al. 2003).

Results

Geochronology

Age model

The age model for the upper part of the core is based on 49 radiocarbon ages and paleosecular variation dates for the bottom 7 m of the core, which did not contain any organic material to facilitate radiocarbon dating of the sediments (Fig. 3; Tables 1, 2). An age model was developed by dividing the core into four sections based on the changing lithofacies and varve thicknesses and using a piece-wise linear regression approach (Telford et al. 2004).

Two wood samples (UCIAMS 2288, 2289) at 2161 cm depth yielded ages that differed by only 60 ^{14}C years BP (60 cal. years BP, Table 2), showing that ages from plant material are quite reliable as indicators of sediment age. We elected to base the age model solely on the terrestrial materials because the results for the nine contemporaneous shell samples (UCIAMS 2296–2304) were badly scattered ranging from 9290 ± 35 ^{14}C years BP (9040 cal. years BP) to 12 940 ± 60 ^{14}C years BP (12 470 cal. years BP, Table 2).

The core spans the time period from 14 360 ^{14}C years BP (17 300 cal. years BP) to 930 ^{14}C years BP (860 cal. years BP; Fig. 3), indicating that ∼2.5 m of sediment is missing from the top of the core, no doubt because of the force of the coring method. All radiocarbon ages, with the exception of three outliers, are in stratigraphic sequence, indicating little sediment disturbance after deposition. The three ages not in stratigraphic sequence (UCIAMS 5741, 10353, 10361,

Fig. 3. Age model for the core based on 49 radiocarbon dates, the Mazama Ash, and correlations of paleomagnetic secular variation features for the bottom 7 m of the core. Sedimentation rates estimated from varve counting appear as varve mm/year. Age likelihood curves are plotted for the calibrated calendar ages.

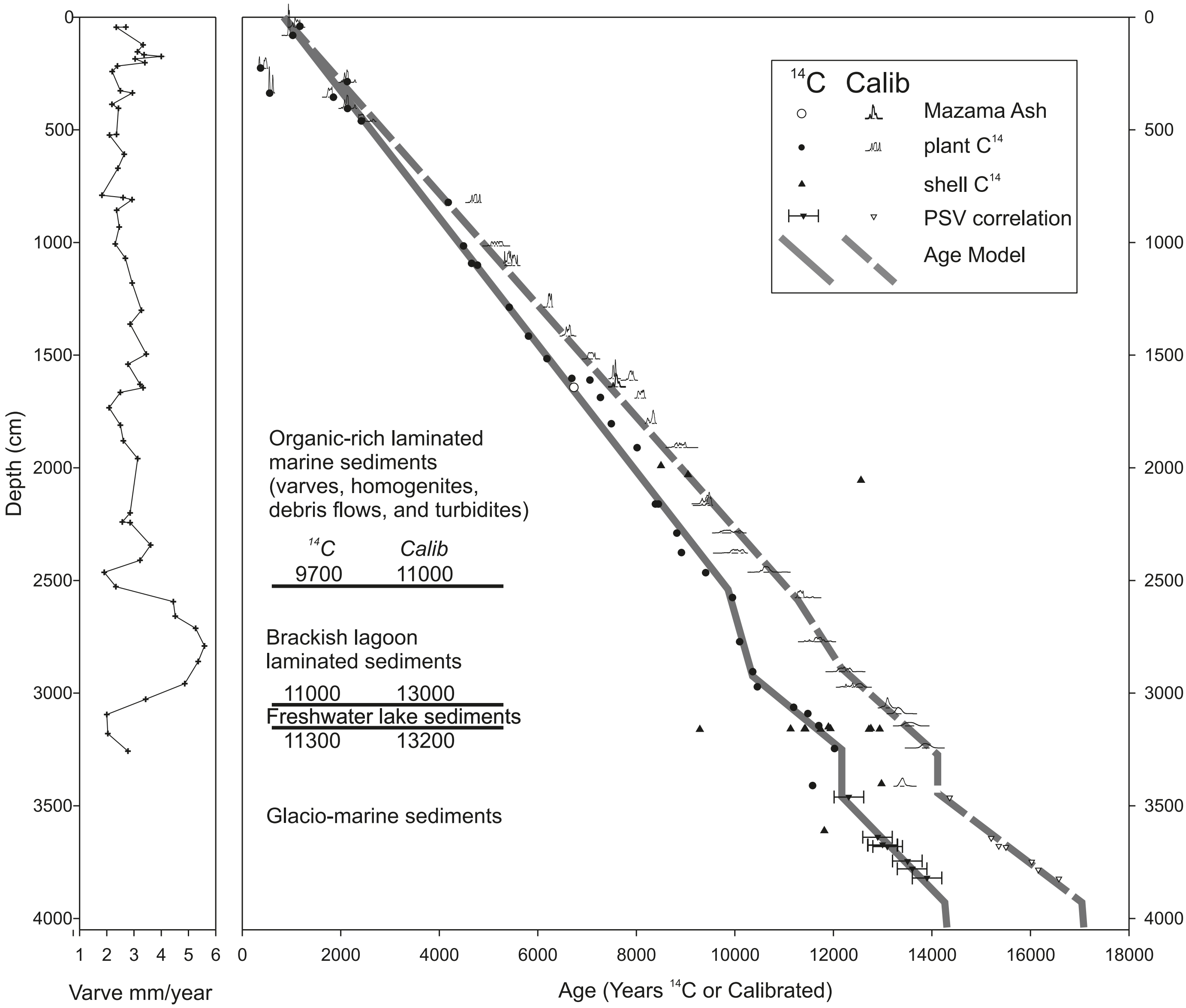

Table 1. MD02-2494 age model.

Depth top (cm)	Depth bottom (cm)	^{14}C years/cm	^{14}C mm/year	^{14}C years intercept	Cal. years/cm	Cal. mm/year	Cal. intercept	*n*
0	2500	3.521	2.84	925	4.067	2.46	855	25
2500	3000	1.304	7.67	6555	2.886	3.47	3831	4
3000	3300	5.661	1.77	–6201	5.085	1.97	–2515	5
3300	4092	2.77	3.61	3020	4.061	2.46	686	(7 psv)

Note: Cal., calibrated; *n*, number of dates; psv, dates from paleosecular variation correlation.

Table 2) were classified as outliers and not included in the age model because of the possibility that these samples, particularly UCIAMS 5741 and 10353, which are younger than the surrounding sediment, were dragged down the side of the core during penetration of the core barrel.

No organic material was found below 3611 cm in the core, leaving the ice-distal and ice-proximal sediments without dating control. However, comparing the seven paleomagnetic secular variation features from this part of the core with North American paleosecular variation curves for the Late Pleistocene (Lund et al. 1988; Dallimore et al. 2005*b*) indicates that deposition in Effingham Inlet started

Table 2. Radiocarbon dating results.

Depth (cm)	Age (^{14}C years BP)	Calibrated age (cal. years BP)	Laboratory number	Dated material	Lithofacies and setting
41	1170±25	1097±44	10352	Moss	Laminated, anoxic marine
81	1025±20	940±10	2226	Wood	Laminated, anoxic marine
226	**370±20**	**415±72**	5741	Twig	Laminated, anoxic marine
286	2130±20	2105±42	5742	Bark	Homogenite, anoxic marine
338	**555±21**	**575±35**	10353	Twig	Laminated, anoxic marine
356	1850±20	1780±42	2227	Cone	Laminated, anoxic marine
406	2135±20	2112±42	2228	Wood	Laminated, anoxic marine
461	2415±20	2415±56	2229	Plant	Laminated, anoxic marine
822	4180±20	4731±87	5746	Bark	Laminated, anoxic marine
1016	4490±25	5184±115	2230	Plant	Homogenite, anoxic marine
1093	4655±20	5399±64	2231	Wood	Laminated, anoxic marine
1101	4775±25	5519±55	2232	Wood	Laminated, anoxic marine
1288	5420±20	6238±40	5747	Twig	Laminated, anoxic marine
1416	5810±25	6617±48	2233	Plant	Homogenite, anoxic marine
1516	6185±25	7078±72	2234	Plant	Homogenite, anoxic marine
1603	6690±30	7545±38	2235	Wood	Laminated, anoxic marine
1610	7055±35	7886±70	2236	Plant	Laminated, anoxic marine
1688	7270±20	8091±66	5748	Charcoal	Laminated, anoxic marine
1804	7490±25	8291±70	5749	Wood	Laminated, anoxic marine
1911	8015±40	8899±114	2284	Wood	Laminated, anoxic marine
1991	8500±30	8737±124	2285	Shell	Debris flow, anoxic marine
2031	9050±35	9262±204	2286	Shell	Debris flow ,anoxic marine
2056	12560±60	13787±272	2287	Shell	Debris flow, anoxic marine
2161*	8445±40	9480±46	2288	Wood	Debris flow, anoxic marine
2161*	8385±40	9421±80	2289	Wood	Debris flow, anoxic marine
2290	8820±50	9880±210	2290	Wood	Disturbed laminated, anoxic marine
2376	8915±50	10032±120	2291	Plant	Homogenite
2466	9405±50	10625±66	2292	Plant	Laminated, anoxic marine
2576	9950±25	11327±54	2576	Twig	Laminated, anoxic marine
2772	10095±30	11588±155	2772	Twig	Laminated, anoxic marine
2905	10360±25	12179±158	2905	Twig	Laminated, anoxic marine
2972	10455±30	12340±189	2972	Twig	Laminated, anoxic marine
3063	11190±30	13016±90	10359	Twig	Laminated, freshwater lake
3091	11480±60	13402±295	2293	Twig	Laminated, freshwater lake
3144*	11900±60	13141±191	2295	Shell	Marine–freshwater transition
3158*	12760±60	14055±239	2296	Shell	Marine–freshwater transition
3158*	11940±50	13176±183	2297	Shell	Marine–freshwater transition
3159*	11130±45	12304±338	2230	Shell	Marine–freshwater transition
3159*	11430±45	12716±258	2299	Shell	Marine–freshwater transition
3159*	11415±50	12692±262	2300	Shell	Marine–freshwater transition
3160*	12940±60	14396±605	2301	Shell	Marine–freshwater transition
3160*	11740±50	13016±125	2302	Shell	Marine–freshwater transition
3161*	12720±60	13982±311	2303	Shell	Marine–freshwater transition
3161*	9290±35	9638±184	2304	Shell	Marine–freshwater transition
3245	12020±70	14021±234	2305	Wood	Laminated, glacimarine
3402	12975±30	15012±461	10360	Shell	Laminated, glacimarine
3410	**11575±30**	**13334±96**	10361	Wood	Lminated, glacimarine
3611	11815±50	13041±129	2306	Shell	Clay, glacimarine

Note: Bold dates are classified as outliers; dates with * are contemporaneous.

~14 360 ^{14}C years BP (17 300 cal. years BP), which is compatible with the estimated age of initial deglaciation in the area (Clague 1989, 1994; Ward 2003).

Mazama Ash

The Mazama Ash was identified in hand sample as a thin (0.5 cm), light grey ash layer at 1646 cm in the core. The ash was positively identified by electron microprobe at the University of Toronto (J. Westgate, personal communication, 2005), Toronto, Ontario. This is the most northwesterly occurrence of the Mazama Ash reported to date (cf. Hutchinson et al. 2004*a*) and anchors the age model of the core sediments at 1646 m (Fig. 3). The accepted date for the ash, 6730 ^{14}C years BP (Hallett et al. 1997), agrees well

Fig. 4. Representative lithofacies from core photographs and X-radiographs. (A) Ice-proximal sediments showing coarse-grained sand lenses. (B) Ice-distal glacimarine unit A (iceberg zone) sediments with finer grained sand and silt laminations than the underlying ice-proximal sediments. (C) Ice-distal glacimarine unit B sediments with X-rays showing developing diatomaceous, silt, and mud varves suggesting deposition in an anoxic environment. (D) Shallow marine basin unit sediments showing pale yellow coloring and clay, silt, and diatomaceous varves. (E) Marine–freshwater transition unit sediments showing erosive lower contact and shells and pebbles in clay matrix. (F) Freshwater lake sediments and X-rays showing finely laminated diatomaceous, silt, and mud varves. (G) Shallow marine, brackish water sediments and X-rays showing thickest diatomaceous and terrigenous varves of the core. A homogenite is visible from 2641 to 2646 cm.

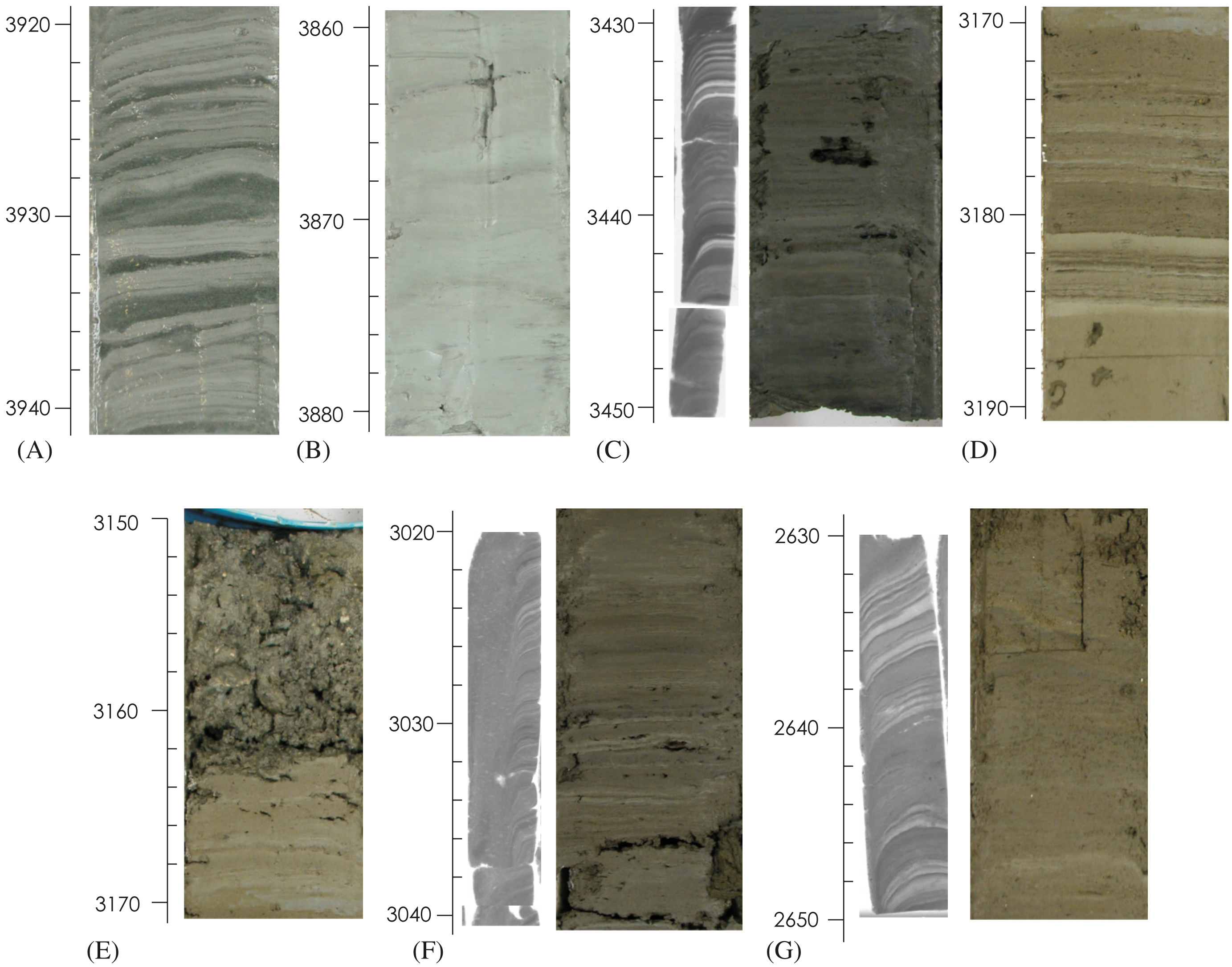

with our calculated age of 6720 ^{14}C years BP (7550 cal. years BP) based on the age model for the core sediments at 1646 cm.

Three other potential ash layers were found in the core sediments at 1342, 2346, and 2356 cm. However, microprobe analyses showed although the samples are composed of glass shards, they are too fine grained for a determination of a glass composition from a 6 μ wide beam and, therefore, were not positively identified (J. Westgate, personal communication, 2005). The age model shows, if these are tephra, the events would have occurred at ∼5650 ^{14}C years BP (6310 cal. years BP), 9190 ^{14}C years BP (10 400 cal. years BP), and 9220 ^{14}C years BP (10 440 cal. years BP) and may possibly be related to Holocene eruptions from Cascadia vents. However, no eruptions at these times have been reported in the literature (Hickson et al. 1999).

Sedimentology and micropaleontology

The main lithofacies in the core were classified by a combination of sedimentology, micropaleontology, and physical properties measurements (Figs. 3–5). Detailed sedimentology, micropaleontology, photographs, and X-radiographs of the core sediments can be found in Dallimore et al. 2008. The vertical sequence of lithofacies was compared with contemporaneous deglacial sediments described from the Georgia Basin (Barrie and Conway 2002*b*) and with the lateral progression of sediments accumulating in the present day along the length of Tarr Inlet, Alaska, where a tidewater glacier has been actively retreating with several hiatuses and readvances in the last few centuries (Cai et al. 1997).

The basal lithofacies succession in the core shows that Effingham Inlet evolved from a somewhat restricted glacimarine embayment shortly after ice began to recede. A brief

Fig. 5. Density, magnetic susceptibility (SI units) measurements, and colour (hue) of the core. Compare changes in physical properties to lithofacies changes identified in the left column. Seismites and debris flows are indicated by shaded bars. The high values of susceptibility in the glacimarine units A and B represent ice-rafted debris in the sediments when the ice front was calving into the inlet. Susc, susceptibility.

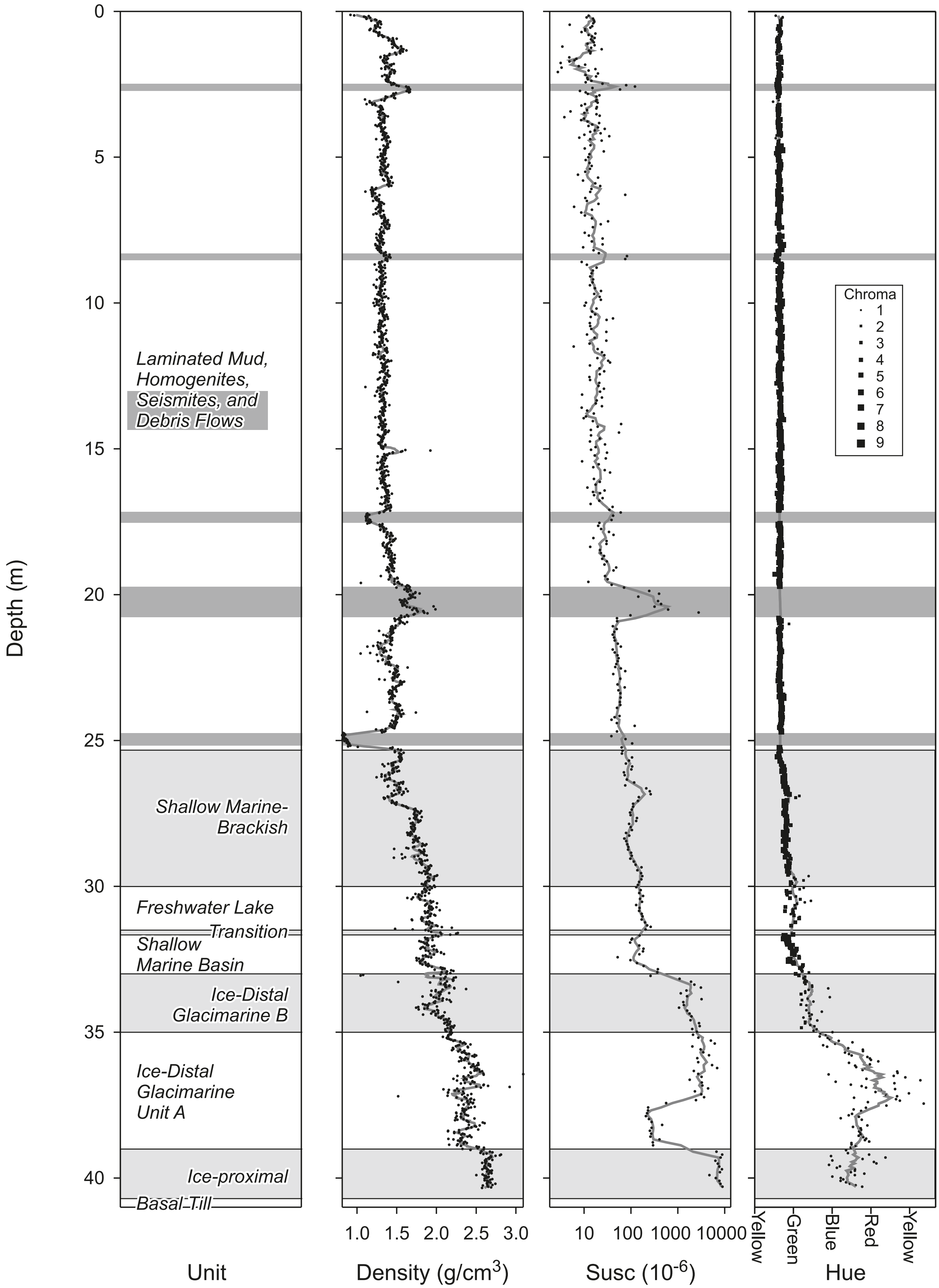

Fig. 6. Sedimentology and magnetic susceptibility (a measure of the concentration of magnetite) of sediments at 750-900 cm depth in the core. The higher values show an increase in clastic material to the sediment column, allowing a differentiation between homogentites and allocthonous seismite lithofacies. Homogenites are remixed, laminated sediments and thus have very similar or equal susceptibility values to laminated sediments whereas seismites have a much higher susceptibility value.

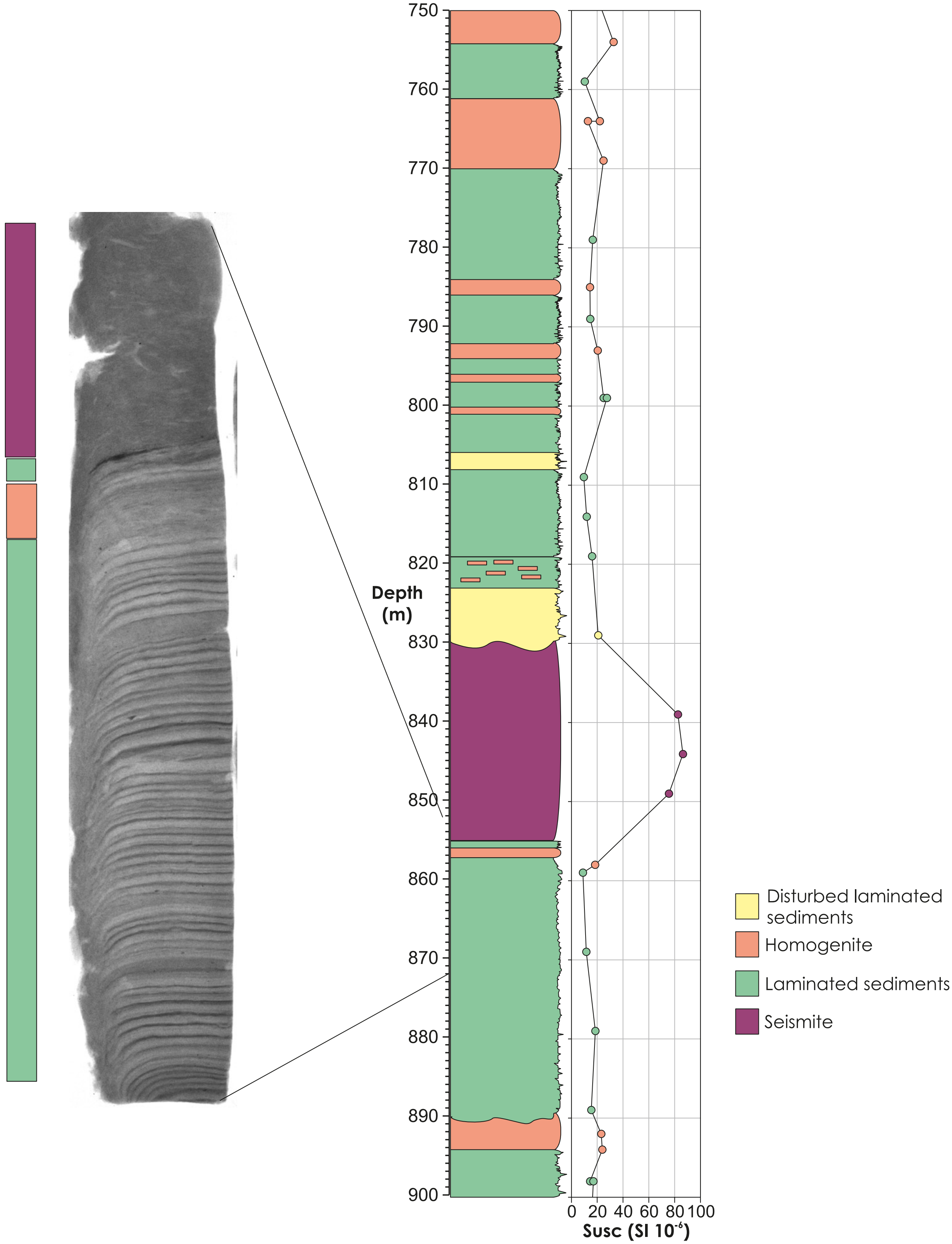

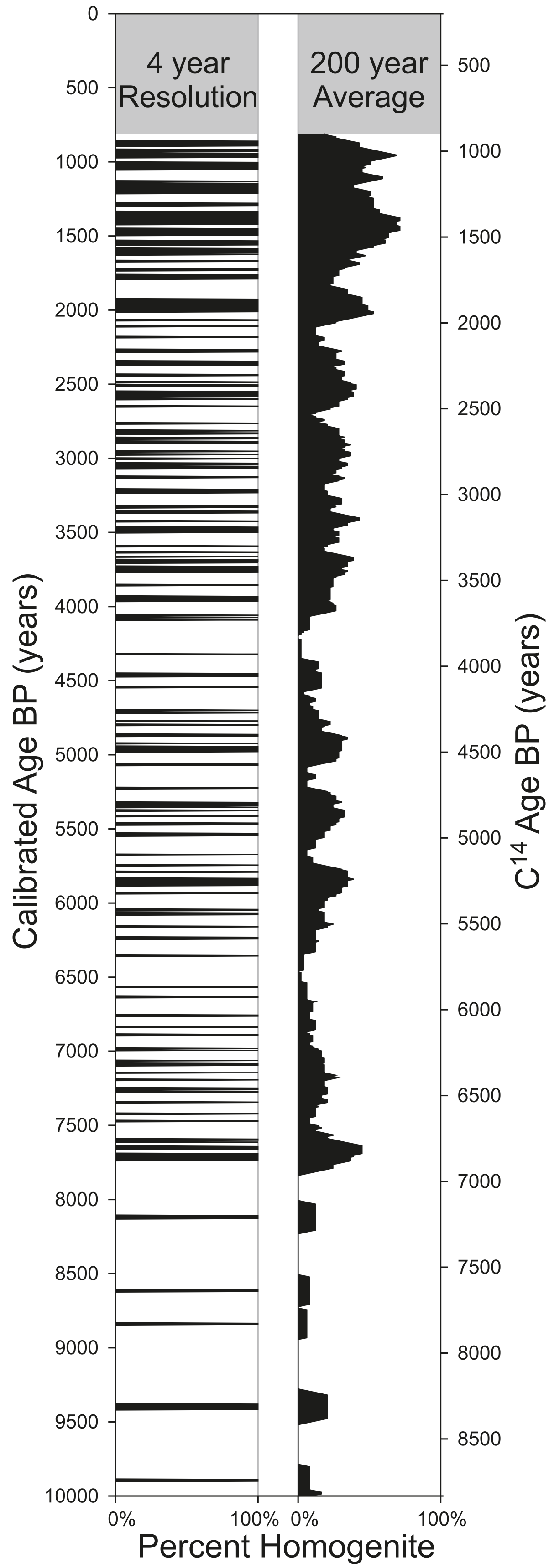

Fig. 7. A running 200-year average of the frequency of homogenite units in the core sediments shows an increase in the frequency of these units throughout the Holocene towards the present. This represents a progressive change in climatic conditions throughout the late Holocene, showing stronger upwelling and greater frequency of large storm events towards the present.

($\sim$850 years) lacustrine phase, identified by the presence of freshwater diatoms, occurred after sea level dropped below the level of the sill $\sim$11 000 ^{14}C years BP. Sea level rose above the sill, and the inlet quickly developed into a highly productive, anoxic marine basin at $\sim$9800 ^{14}C years BP, characterized by the accumulation of laminated (annually varved) diatomaceous silty clays, an environment that is similar to the modern condition. Intercalated at irregular intervals within the laminated sediments in the top 2535 cm of the core are thin ($\sim$<10 cm), unlaminated mud units termed homogenites, which represent remixing of previously laminated sediments (Fig. 6). A 200-year running average of the frequency of these homogenites in this section of the core shows an increase in their occurrence towards the present (Fig. 7).

Also intercalated within the laminated sediments of the core are massive and graded mud units, termed seismites and debris flow units (Fig. 6), which are considered to arise from debris flows and turbidity currents, some of which may have been initiated by seismic events (Dallimore et al. 2005*a*, 2005*b*). These seismites are differentiated from homogenites by their distinctive paleomagnetic signature, which indicates an allocthonous source of these sediments (Fig. 6). Five of the seismites are >10 cm in thickness, and we tentatively interpret them as being the result of sediment failure associated with seismic shaking. These seismites are found at 246–272 cm, 830–855 cm, 1714–1750 cm, 1975–2075 cm, and 2472–2518 cm. According to the age model (Fig. 3), if they have a seismic origin, they would be associated with events that occurred at 1840 ^{14}C years BP (1900 cal. years BP), 3890 ^{14}C years BP (4280 cal. years BP), 7020 ^{14}C years BP (7900 cal. years BP), 8060 ^{14}C years BP (9090 cal. years BP), and 9710 ^{14}C years BP (11 020 cal. years BP), respectively. Disturbed laminated sediments between 2070 and 2215 cm occur just beneath one of the seismites (1974–2070 cm), which is a fluid and highly disturbed, olive grey clay with a distinctive magnetic signature (Fig. 5). This unit may represent a large gas void, possibly supporting the inference for seismic shaking of the sea floor at this time (Dallimore et al. 2005*a*).

Discussion

Age model

The number of dates in the Holocene section of the core is unusually high, with 49 radiocarbon dates over 40.9 m of core. Telford et al. (2004) modelled an ideal theoretical fit of radiocarbon dates to a varved Holocene section and concluded that a best fit age model with a high degree of certainty can be obtained with 24 radiocarbon dates over the length of a Holocene section, which they point out is in fact rarely a possibility in actual practice. The core has twice as many dates as the ideal theoretical model of Telford's, with 49 dates over a Holocene section and, therefore, the high

Fig. 8. Relative sea-level curve for the Barkley Sound region, showing ages from the late Pleistocene marine–freshwater–brackish–marine succession, which is plotted at the present sill depth of 46 m below present sea level. Younger ages on the curve are from a compilation of dated archeological and geological material from around Barkley Sound, as compiled by Hutchinson (1992). The inferred relative sea-level curve (broken line) is the difference between the global eustatic sea-level curve (thick line) and the local elevation changes (crustal response) caused by modelled tectonics and isostatic effects (thin line). The ages of materials are calibrated ^{14}C dates because the crustal response decay times are estimated in real years; the ^{14}C age scale at the top of the graph is approximate and given for reference.

statistical confidence in the age model could render it useful as a geochronological tie-point or scale for other sedimentary records on the northeast Pacific coast. If the sequential pattern of varved sediments and abrupt changes in the paleoclimatic signal or sediment disturbances contemporaneous with the seismites identified in the core can be found elsewhere, this age model could be used to help date and identify those records and events.

Paleosecular variation dating

A comparison of changes in paleosecular variation measurements with reference poles in North America has not been well established for the Holocene and late Pleistocene. However, these variations are known to occur on time scales of centuries to millennia, and their presence in the lower part of the core represents the passage of time during the deposition of the proglacial and ice-proximal sediments. In deglacial fjord settings, sediment can be delivered to the basin chaotically from multiple provenances in the upper part of the glacial valley as ice recedes; this could also complicate the magnetic signal, making it perhaps not directly comparable to paleosecular variation Holocene records from other, more stable environmental settings such as lakes. We propose seven correlations with the paleosecular curves of Mono Lake, California (Lund et al. 1988).

Sedimentation rates for the ice-proximal and ice-distal sediments estimated from the paleosecular variation age estimates are probably too low compared with the modern analogue of the depositional pattern in Tarr Inlet, Alaska (Cai et al. 1997). The basal date of the core seems accurate however, based on the known time of deglaciation on this coast. Underestimates of sedimentation rates in the glacial sediments, interpreted from counting of sand lenses in the ice-proximal sediments and comparison with sedimentation rates from contemporaneous sediments in Georgia Basin, may indicate that there was a lengthy depositional hiatus at a time when the core site was subice — before a period of only a few centuries when rapid ice-proximal and ice-distal sedimentation was occurring, as was the case in the Strait of Georgia to the east (Barrie and Conway 2002*a*, 2002*b*).

Sea-level change

Local relative sea-level observations plotted against a eustatic sea-level curve yield an estimated best fit isostatic depression curve describing local mantle response to loading and unloading (James et al. 2005). For the west coast of Vancouver Island, we have plotted the relative sea-level observations from Effingham Inlet and areas around Barkley Sound (map areas 3 and 5, Hutchinson 1992) against the Barbados eustatic sea-level curve (Fairbanks 1989; Bard et al. 1996; Stanford et al. 2006). The freshwater period in Effingham Inlet, when the inlet was an "isolation basin" (Hutchinson et al. 2004*a*), constrains our new local sea-level curve setting a precise lowstand of sea level in this area at 46 m below present datum, ~11 630 ^{14}C years BP (13 500 cal. years BP), when the sill was subaerially exposed (Figs. 8, 9). The transition from sediments containing freshwater diatoms to brackish water diatoms occurs at 11 075 ^{14}C years BP (13 000 cal. years BP), marking a gradual breach of the sill. At 9850 ^{14}C years BP (11 125 cal. years), near the time of meltwater pulse 1B (Fig. 8), sea level rose over the sill once more and the lake became an anoxic marine inlet.

The sea-level curve also shows that glacially induced isostatic rebound ceased ~4500 ^{14}C years BP when sea level stabilized a few metres above present. Since that time, sea level in the Barkley Sound area has been falling slowly, which is thought to have been induced by tectonic crustal uplift of ~0.5 mm/year rather than isostatic rebound. Estimates from Georgia Basin give a present-day crustal uplift rate due to the residual isostatic effects of the Cordilleran Ice Sheet of ~0.25 mm/year (James et al. 2005).

James et al. (2002, 2005) show that variable mantle response to isostatic unloading along the Cascadia subduction zone is composed of an earlier response controlled by the low-viscosity upper mantle and a later response controlled by the more viscous lower mantle. The same two part mantle response is found in the Barkley Sound area. The crustal reponse curve, which is modelled by fitting the relative sea-level data to an exponential curve, is composed of two exponential decay terms with characteristic decay times of 500 and 2600 years (Fig. 8). These values are the same as those inferred from sea-level observations in the northern Strait of Georgia (James et al. 2005). Two decay times are needed because no single exponential curve fits the isolation basin dated sequence adequately, reflecting a variable mantle response at different times during deglaciation. The rapid decay time constant is also necessary because local relative sea level was dropping at the same time that meltwater pulse 1A was increasing the rate of global sea-level rise. The change in direction of the sea-level curve (Fig. 8) (sea-level rising to sea-level falling) is controlled by the change in slope in the eustatic sea-level curve at 4500 ^{14}C years BP, whereas data from the Barkley Sound region suggest that this transition occurred earlier, at ~7000–8000 ^{14}C years BP.

The new sea-level curve shows that the lowstand in Effingham Inlet at ~11 630 ^{14}C years BP (13 500 cal. years BP) occurred ~1000 years earlier than the lowstand in the Georgia Basin, 100 km to the east (James et al. 2005). Although the magnitude of the lowstand in Effingham Inlet (~50 m) was about the same as in the Georgia Basin (Barrie and Conway 2002*a*, 2002*b*), the amount of crustal depression was different. This is because eustatic sea level was lower during the Effingham Inlet lowstand than during the later lowstand in the Georgia Basin. Crustal isostatic depression was highly variable immediately following deglaciation and was ~230 m in the Georgia Basin, in contrast to

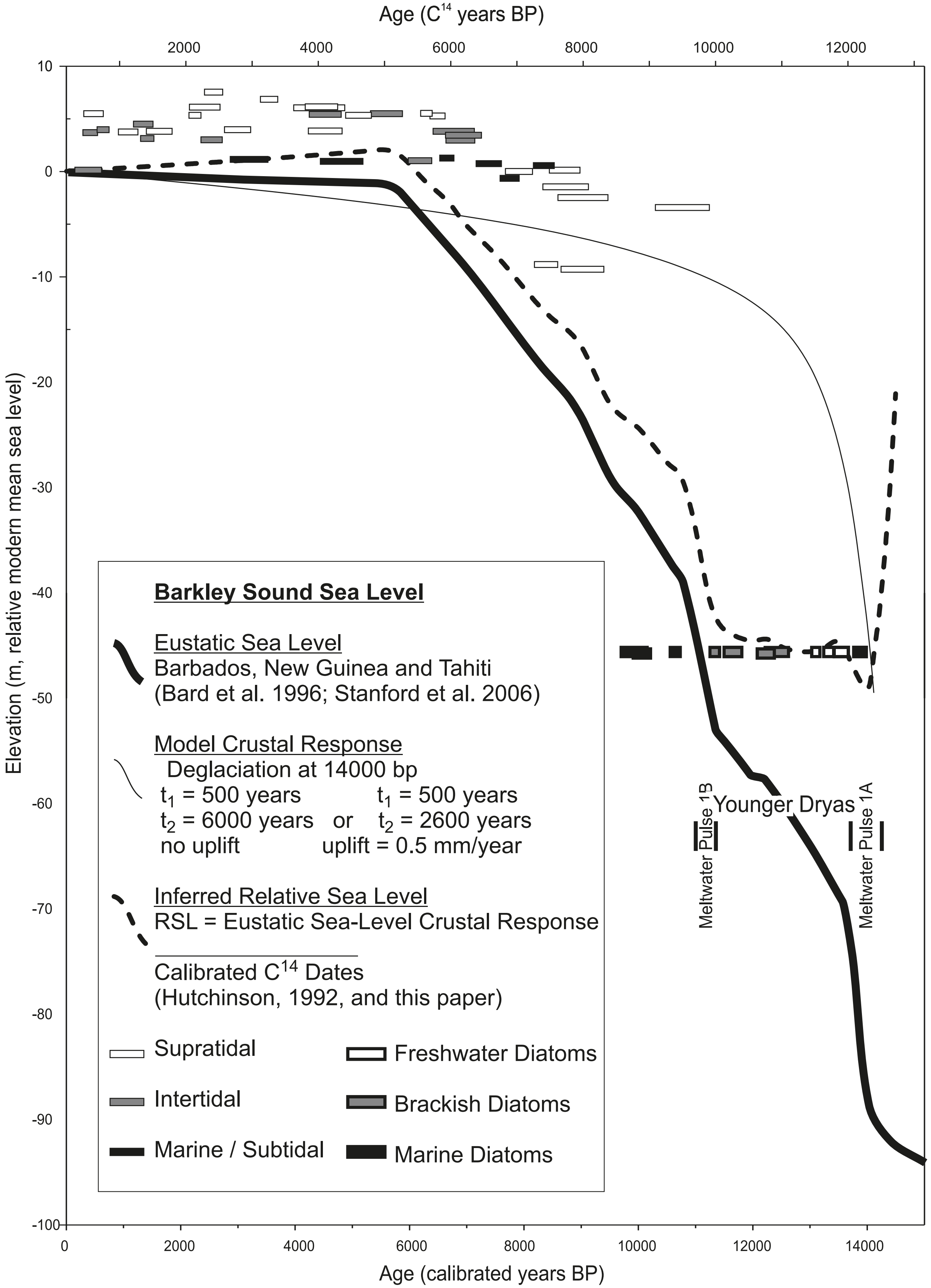
Age (C14 years BP)
2000
4000
6000
8000
10000
12000
Elevation (m, relative modern mean sea level)
10
0
-10
-20
-30
-40
-50
-60
-70
-80
-90
-100
Barkley Sound Sea Level
Eustatic Sea Level
Barbados, New Guinea and Tahiti
(Bard et al. 1996; Stanford et al. 2006)
Model Crustal Response
Deglaciation at 14000 bp
t1 = 500 years
t2 = 6000 years or
no uplift
t1 = 500 years
t2 = 2600 years
uplift = 0.5 mm/year
Inferred Relative Sea Level
RSL = Eustatic Sea-Level Crustal Response
Calibrated C14 Dates
(Hutchinson, 1992, and this paper)
Supratidal
Intertidal
Marine / Subtidal
Freshwater Diatoms
Brackish Diatoms
Marine Diatoms
Meltwater Pulse 1B
Younger Dryas
Meltwater Pulse 1A
0
2000
4000
6000
8000
10000
12000
14000
Age (calibrated years BP)

Fig. 9. Detail of boxed inset area from Fig. 1: (A) showing bathymetry of Barkley Sound today and (B) bathymetry of Barkley Sound 11 000 years ago when sea level was ∼46 m lower than present.

*30 m in Effingham Inlet (James et al. 2005; T. James, personal communication, 2006). This is perhaps an indication of a thicker and more persistent ice load in the Georgia Basin, which lasted for ∼1000 years longer than the ice load in the Effingham Inlet area, creating a larger crustal depression. A proglacial forebulge might be expected in the Georgia Basin but there has been no conclusive evidence of one reported (Hetherington and Barrie 2004).

Holocene paleoceanographic changes

Thick ice in the Juan de Fuca Strait around the southern end of Vancouver Island separated the Georgia Basin from the relatively warmer waters of the open ocean circulation at initial deglaciation (Barrie and Conway 2002*a*, 2002*b*). The Juan de Fuca Strait (Fig. 1), which today is connected to Barkley Sound and related to the coastal ocean conditions to the west of Vancouver Island (Hay et al. 2007), was the first part of the area that was ice-free and open to the Pacific Ocean and experiencing glacimarine sedimentation by ~13 500 ^{14}C years BP (16 250 cal. years BP). Open marine conditions were then soon established in the Georgia Basin ~12 400 ^{14}C years BP (14 250 cal. years BP), signalling fully marine circulation around Vancouver Island about that time (Howes 1983; Barrie and Conway 2002*a*, 2002*b*).

In Effingham Inlet, the upper glacimarine unit contains finely laminated sediments with a shallowing sill at ~30 m water depth. This suggests that modern conditions of bottom water anoxia and restricted open ocean circulation with a shallow Barkley Sound were established at about the same time as open marine conditions existed all around the island, at ~12 500 – 13 000 ^{14}C years BP (14 250 – 15 500 cal. years BP). Open marine circulation to the north in Dixon Entrance was also established about this time, at 13 000 ^{14}C years BP (15 500 cal. years BP; Guilbault et al. 1997), indicating that modern oceanographic conditions and coastal ocean dynamics were established by the earliest Holocene.

It appears that stormy, extreme weather conditions have become more frequent in Barkley Sound since ~10 200 ^{14}C years BP (11 900 cal. years BP) when the sill was at ~20 m depth, when homogenite lithofacies first appear in the core. Homogenites result from the reworking of previously laminated sediments by dense bottom currents triggered by strong episodes of upwelling that in turn are prompted by extreme storm conditions (Dallimore et al. 2005*a*; Hay et al. 2007). A 200-year running average of the occurrence of massive homogenite units (Fig. 7) shows that these stormy, extreme weather conditions (Dallimore et al. 2005*a*) have become more frequent in the coastal ocean throughout the Holocene.

Conclusions

Holocene and late Pleistocene sediments preserved in the new MD02-2494 core record conditions in the inlet as glaciers receded beginning ~14 000 ^{14}C years BP. Once deglaciation of Effingham Inlet began, it proceeded rapidly without major stillstands and re-advances, indicating a warming late Pleistocene climate. Modern coastal ocean dynamics were established around Vancouver Island ~10 000 ^{14}C years BP (11 500 cal. years BP), once the effects of the Fraser Glaciation had waned and an increase in storminess and wind fields increased throughout the Holocene to the present. Modern oceanographic conditions creating bottom water anoxia were established in Effingham Inlet ~10 000 ^{14}C years BP.

Effingham Inlet experienced a sea-level fall and then a rise of almost 50 m because of eustatic and isostatic crustal adjustments that persisted from ~11 000 to 4500 ^{14}C years BP. This crustal adjustment, combined with rising global eustatic sea-level change, resulted in the inner basin of the inlet becoming a freshwater lake for ~850 years at ~11 600 ^{14}C years BP (13 500 cal. years BP) when the sill, which today is at 46 m depth, became briefly subaerially exposed. The timing of the sea-level lowstand when Effingham Inlet was an isolation basin provides the two index points needed for a new sea-level curve for the outer coast of Vancouver Island. A variable mantle response to deglaciation is indicated, composed of an early response controlled by the low-viscosity upper mantle and a later response controlled by a more viscous lower mantle.

The laminated sediments preserved in the inlet since ~10 000 ^{14}C years BP also record possible seismic events along the Cascadia subduction zone that may have occurred ~1840 ^{14}C years BP (1900 cal. years BP), 3890 ^{14}C years BP (4280 cal. years BP), 7020 ^{14}C years BP (7900 cal. years BP), 8060 ^{14}C years BP (9090 cal. years BP), and 9710 ^{14}C years BP (11 020 cal. years BP). Volcanic ash layers in the cores may be products of unrecorded eruptions from Cascadia vents at ~5650 ^{14}C years BP (6310 cal. years BP), 9190 ^{14}C years BP (10 400 cal. years BP), and 9220 ^{14}C years BP (10 440 cal. years BP).

The MD02-2494 core is currently the best-dated Holocene record for the northeastern Pacific. The resulting high-resolution analyses of the sediment properties reported here and in Ivanochko et al. 2008 serve as a chronological and event-based tie point and comparison for other paleoenvironment records of the northeastern Pacific.

Acknowledgments

We extend our gratitude for the support of the International Marine Global Changes Program and Past Global Changes Program, and Chief Scientist, Dr. Beaufort, as well as the captain and crew of the *RV Marion Dufresne.* The core data were analyzed with funding contributed by the Canadian Foundation for Atmospheric Sciences for the Polar Climate Stability Network highlighted in this special issue. Our thanks to Dr. Ralph Currie and Dr. Phil Hill for their continued support of this work at Natural Resources Canada, and Dr. Jim Bayer and Dr. Tony Boydell of Royal Roads University for their support. Dr. Tom James, Natural Resources Canada, and Dr. Murray Hay, Université Laval, were instrumental with their intellectual contribution to the manuscript and are much appreciated, as are the thoughtful comments of reviewers Dr. Vaughn Barrie, Natural Resources Canada, Dr. Ian Hutchison, Simon Fraser University, and Dr. Pete Hollings, Associate Editor of the Canadian Journal of Earth Sciences. Our thanks also to student Mischa Macdonald who helped with the ash lithofacies identification.

References

Axelsson, V. 2002. Monitoring sedimentation by radiographic core-to-core correlation. Geo-Marine Letters, **21**: 236–244. doi:10.1007/s00367-001-0084-4.

Bard, E., Hamelin, B., Arnold, M., Montaggioni, L.F., Cabioch, G., Faure, G., and Rougerie, F. 1996. Deglacial sea-level record from Tahiti corals and the timing of global meltwater discharge. Nature, **382**: 241–244. doi:10.1038/382241a0.

Barrie, J.V., and Conway, K.W. 1999. Late Quaternary glaciation and postglacial stratigraphy of the northern Pacific margin of Canada. Quaternary Research, **51**: 113–123. doi:10.1006/qres.1998.2021.

Barrie, J.V., and Conway, K.W. 2002*a*. Rapid sea-level change and coastal evolution on the Pacific margin of Canada. Sedimentary Geology, **150**: 171–183. doi:10.1016/S0037-0738(01)00274-3.

Barrie, J.V., and Conway, K.W. 2002*b*. Contrasting glacial sedimentation processes and sea-level changes in two adjacent basins on the Pacific margin of Canada. *In* Glacier-influenced sedimentation on high-latitude continental margins. *Edited by* J.A. Dowdeswell and C. O'Cofaigh. Geological Society, London, Special Publications 203, pp. 181–194.

Beaufort, L. 2002. Les rapports de campagnes à la mer MD126/ MONA Marges Ouest Nord Américaines IMAGES VIII à bord du Amrion Dufresne. Réf: OCE/2002/03. Insitute Polaires Français, Plouzané, France. Available from www.images-pages.org [accessed 15 March 2008].

Cai, J., Powell, R.D., Cowan, E.A., and Carlson, P.R. 1997. Lithofacies and seismic-reflection interpretation of temperate glacimarine sedimentation in Tarr Inlet-Glacier Bay, Alaska. Marine Geology, **143**: 5–37. doi:10.1016/S0025-3227(97)00088-1.

Campeau, S., Pienitz, R., and Héquette, A. 1999. Diatoms from the Beaufort Sea Coast, Southern Arctic Ocean (Canada). *In* Bibliotheca diatomologica, Vol. 42. J. Cramer, Berlin and Stuttgart, Germany.

Chang, A.S., Patterson, R.T., and McNeely, R. 2003. Seasonal sediment and diatom record from the late Holocene laminated sediments, Effingham Inlet, British Columbia, Canada. Palaios, **18**: 477–494. doi:10.1669/0883-1351(2003)018<0477:SSADRF>2.0.CO;2.

Clague, J.J. 1981. Late Quaternary geology and geochronology of British Columbia. Part 2: Summary and discussion of radiocarbon-dated Quaternary history. Geological Survey of Canada, Paper 80-35.

Clague, J.J. 1983. Glacio-isostatic effects of the Cordilleran Ice Sheet, British Columbia, Canada. *In* Shorelines and isostacy. *Edited by* D.E. Smith and A.G. Dawson. Institute of British Geographers, Special Publication 16, pp. 321–343.

Clague, J.J. 1989. Cordilleran ice sheet. *In* Quaternary geology of Canada and Greenland. Vol. 1. *Edited by* R.J. Fulton. Geological Survey of Canada, Ottawa, Ont., pp. 40–42.

Clague, J.J. 1994. Quaternary stratigraphy and history of south-coastal British Columbia. *In* Geology and geological hazards of the Vancouver region, southwestern British Columbia. *Edited by* J.W. Monger. Geological Survey of Canada, Bulletin 481, pp. 181–192.

Clague, J.J., and James, T.S. 2002. History and isostatic effects of the last ice sheet in southern British Columbia. Quaternary Science Reviews, **21**: 71–87. doi:10.1016/S0277-3791(01)00070-1.

Clague, J.J., Harper, J.R., Hebda, R.J., and Howes, D.E. 1982. Late Quaternary sea-levels and crustal movements, coastal British Columbia. Canadian Journal of Earth Sciences, **19**: 597–618. doi:10.1139/e82-048.

Dallimore, A. 2001. Late Holocene geologic, oceanographic and climate history of an anoxic fjord: Effingham Inlet, Vancouver Island. Ph.D. thesis, Department of Earth Sciences, Carleton University, Ottawa, Ont.

Dallimore, A., Thomson, R.E., and Bertram, M.A. 2005*a*. Modern to Late Holocene deposition in an anoxic fjord on the west coast of Canada: implications for regional oceanography, climate and paleoseismic history. Marine Geology, **219**: 47–69. doi:10.1016/j.margeo.2005.05.003.

Dallimore, A., Enkin, R.J., and Southon, J.R. 2005*b*. Post-glacial and paleo-environmental history of the west coast of Vancouver Island. *In* Program and abstracts of the American Geophysical Union, San Francisco, California, 5–9 December 2005. Abstract PP31A-1507.

Dallimore, A., Enkin. R.J., Baker, J., and Pienitz, R. 2008. Stratigraphy and late Holocene history of Effingham Inlet, B.C. Results from MONA core MD02-2494. Geological Survey of Canada, Open File 5930.

Enkin, R.J., Baker, J., Norgalieu, D., Iassonov, P., and Hamilton, T.S. 2007. Magnetic hysteresis parameters and day plot analysis to characterize diagenetic alteration in gas hydrate-bearing sediments. Journal of Geophysical Research, **112**(B6): No. B06S90.

Fairbanks, R.G. 1989. A 17,000 year glacio-eustatic sea-level record; influence of glacial melting rates on the Younger Dryas event and deep-ocean circulation. Nature, **342**: 637–642. doi:10.1038/342637a0.

Fedje, D., and Josenhans, H.W. 2000. Drowned forests and archaeology on the continental shelf of British Columbia, Canada. Geology, **28**: 99–102. doi:10.1130/0091-7613(2000)28<99:DFAAOT>2.0.CO;2.

Fisher, D.A., Wake, C., Kreutz, K., Yalcin, K., Steig, E., Mayewski, P., et al. 2003. Stable isotope records from Mount Logan, Eclipse ice cores and nearby Jelly Bean Lake. Water cycle of the North Pacific over 2,000 years and over five vertical kilometers: sudden shifts and tropical connections. Géographie physique et Quaternaire, **58**: 337–352.

Friele, P.A., and Hutchinson, I. 1993. Holocene sea-level change on the central west coast of Vancouver Island, British Columbia. Canadian Journal of Earth Sciences, **30**: 832–840. doi:10.1139/e93-069.

Goldfinger, C., Nelson, C.H., and Johnson, J. 2003*a*. Holocene Earthquake Records From the Cascadia Subduction Zone and Northern San Andreas Fault Based on Precise dating of Offshore Turbidites. Annual Reviews of Earth and Planetary Science, **31**: 555–577. doi:10.1146/annurev.earth.31.100901.141246.

Goldfinger, C., Nelson, C.H., and Johnson, J.E. 2003*b*. Deep-Water Turbidites as Holocene Earthquake proxies: The Cascadia Subduction Zone and Northern San Andreas Fault Systems. Annali di Geofisica, **46**: 1169–1194.

Guilbault, J.-P., Patterson, R.T., Thomson, R.E., Barrie, J.V., and Conway, K.W. 1997. Late Quaternary paleoceanographic changes in Dixon Entrance, northwest British Columbia, Canada: Evidence from the foraminiferal faunal succession. Journal of Foraminiferal Research, **27**: 151–174.

Hallett, D.J., Hills, L.V., and Clague, J.J. 1997. New accelerator mass spectrometry radiocarbon ages for Mazama tephra layer from Kootenay National Park, British Columbia, Canada. Canadian Journal of Earth Sciences, **34**: 1202–1209. doi:10.1139/e17-096.

Hay, M.B., Pienitz, R., and Thomson, R.E. 2003. Distribution of diatom surface sediment assemblages within Effingham Inlet, a temperate fjord on the west coast of Vancouver Island (Canada). Marine Micropaleontology, **48**: 291–320.

Hay, M.B., Dallimore, A., Thomson, R.E., Calvert, S., and Pienitz, R. 2007. Siliceous microfossil record of late Holocene oceanography and climate along the west coast of Vancouver Island, British Columbia (Canada). Quaternary Research, **67**: 33–49. doi:10.1016/j.yqres.2006.08.002.

Hebda, R., and Rouse, G.E. 1979. Palynology of two Holocene cores from Hesquiat Peninsula, Vancouver Island, Brisith Columbia. Syesis, **12**: 121–129.

Hetherington, R., and Barrie, J.V. 2004. Interaction between local tectonics and glacial unloading on the Pacific margin of Canada. Quaternary International, **120**: 65–77. doi:10.1016/j.quaint.2004.01.007.

Hetherington, R., Barrie, J.V., Reid, R.G.B., MacLeod, R., Smith, D.J., James, T.S., and Kung, R. 2003. Late Pleistocene coastal paleogeography of the Queen Charlotte Islands, British Columbia, Canada, and its implications for terrestrial biogeography and early postglacial human occupation. Canadian Journal of Earth Sciences, **40**: 1755–1766. doi:10.1139/e03-071.

Hickson, C.J., Russell, J.K., and Stasiuk, M.V. 1999. Volcanology of the 2350 BP eruption of Mount Meager volcanic complex, British Columbia, Canada: implications for hazards from eruptions in topographically complex terrain. Bulletin of Volcanology, **60**: 489–507. doi:10.1007/s004450050247.

Howes, D. 1981. Late Quaternary history of the Hesquiat Harbour Region. M.Sc. thesis, Royal BC Provincial Museum, Victoria, B.C.

Howes, D.E. 1983. Late Quaternary sediments and geomorphic history of northern Vancouver Island, British Columbia, Canada. Canadian Journal of Earth Sciences, **20**: 57–65. doi:10.1139/e83-006.

Hutchinson, I. 1992. Holocene sea-level change in the Pacific Northwest: a catalogue of radiocarbon dates and an atlas of regional sea-level curves. Simon Fraser University, Institute of Quaternary Research, Occasional Paper 1.

Hutchinson, I., James, T.S., Clague, J.J., Barrie, J.V., and Conway, K.W. 2004*a*. Reconstruction of late Quaternary sea-level change in southwestern British Columbia from sediments in isolation basins. Boreas, **33**: 183–194. doi:10.1080/03009480410001299.

Hutchinson, I., James, T., Reimer, P.J., Bornhold, B.D., and Clague, J.J. 2004*b*. Marine and limnic radiocarbon reservoir corrections for studies of late- and postglacial environments in Georgia Basin and Puget Lowland, British Columbia, Canada and Washington, USA. Quaternary Research, **61**: 193–203. doi:10.1016/j.yqres.2003.10.004.

Hyndman, R.D. 1995. Giant earthquakes of the Pacific Northwest. Scientific American, **276**: 1621–1623.

Ivanochko, T.S., Calvert, S.E., Southon, J.R., Enkin, R.J., Baker, J., Dallimore, A., and Pedersen, T.F. 2008. Determining the postglacial evolution of a northeast Pacific coastal fjord using a multiproxy geochemical approach. Canadian Journal of Earth Sciences, **45**: this issue.

James, T.S., Clague, J.J., Wang, K., and Hutchinson, I. 2000. Postglacial rebound at the northern Cascadia subduction zone. Quaternary Science Reviews, **19**: 1527–1541. doi:10.1016/S0277-3791(00)00076-7.

James, T.S., Hutchinson, I., and Clague, J.J. 2002. Improved relative sea-level histories for Victoria and Vancouver, British Columbia, from isolation-basin coring. *In* Current research. Geological Survey of Canada, Paper 2002-A16, 7 p.

James, T.S., Hutchinson, I., Barrie, J.V., Conway, K.C., and Mathews, D. 2005. Relative sea-level change in the northern Strait of Georgia, British Columbia. Geographie physique et Quaternaire, **59**: 113–127

Josenhans, H.W., Fedje, D.W., Conway, K.W., and Barrie, J.V. 1995. Post glacial sea levels on the western Canadian continental shelf: Evidence for rapid change, extensive subaerial exposure, and early human habitation. Marine Geology, **125**: 73–94. doi:10.1016/0025-3227(95)00024-S.

Josenhans, H.W., Fedje, D., Pienitz, R., and Southon, J. 1997. Early humans and rapidly changing Holocene sea-levels in the Queen Charlotte Islands, Hecate Strait, British Columbia, Canada. Science, **277**: 71–74. doi:10.1126/science.277.5322.71.

Kemp, A.E.S. 1996. Laminated sediments as paleo-indicators. *In* Palaeoclimatology and Palaeoceanography from laminated sediments. *Edited by* A.E.S. Kemp. Geolological Society Special Publication 116, p. vii.

Kemp, A.E.S. 2003. Evidence for abrupt climate changes in annually laminated marine sediments. *In* Abrupt climate change; evidence, mechanisms and implications. Papers of a Discussion Meeting. Philosophical Transactions-Royal Society, Mathematical, Physical and Engineering Sciences, **361**: 1851–1870.

Kennett, J.P., and Ingram, B.L. 1995. A 20,000-year record of ocean circulation and climate change from the Santa Barbara Basin. Nature, **377**: 510–514. doi:10.1038/377510a0.

Lund, S.P., Liddicoat, J.C., Lajoie, K.R., Henyey, T.L., and Robinson, S.W. 1988. Paleomagnetic evidence for long-term (10E+4 year) memory and periodic behavior in the earth's core dynamo process. Geophysical Research Letters, **15**: 1101–1104. doi:10.1029/GL015i010p01101.

Luternauer, J.L., Conway, K.W., Clague, J.J., and Blaise, B. 1989*a*. Late Quaternary geology and geochronology of the central continental shelf of western Canada. Marine Geology, **89**: 57–68. doi:10.1016/0025-3227(89)90027-3.

Luternauer, J.L., Clague, J.J., Conway, K.W., Barrie, J.V., Blaise, B., and Mathewes, R.W. 1989*b*. Late Pleistocene terrestrial deposits on the continental shelf of western Canada: evidence for rapid sea-level change at the end of the last glaciation. Geology, **17**: 357–360. doi:10.1130/0091-7613(1989)017<0357:LPTDOT>2.3.CO;2.

Mathews, W.H., Fyles, J.G., and Nasmith, H.W. 1970. Postglacial crustal movements in southwestern British Columbia and adjacent Washington State. Canadian Journal of Earth Sciences, **7**: 690–702. doi:10.1139/e70-068.

McKechnie, I. 2005. Five thousand years of fishing at a shell midden in the Broken Group Islands, Barkley Sound, British Columbia. Ms. thesis, Department of Archaeology, Simon Fraser University, Burnaby, B.C.

Mosher, D.C., and Hewitt, A.T. 2004. Late Quaternary deglaciation and sea-level history of eastern Juan de Fuca Strait, Cascadia. Quaternary International, **121**: 23–39. doi:10.1016/j.quaint.2004.01.021.

Osterberg, E., Mayewski, P., Kreutz, K., Fisher, D., Handley, M., Sneed, S., et al. 2008. Ice core record of rising lead pollution in the north Pacific atmosphere. Geophysical Research Letters, **35**: No. LO5810.

Patterson, R.T., Guilbault, J.-P., and Thomson, R.E. 2000. Oxygen level control of foraminiferal distribution in Effingham Inlet, Vancouver Island, British Columbia. Journal of Foraminiferal Research, **30**: 321–335. doi:10.2113/0300321.

Pienitz, R., Fedje, D., and Poulin, M. 2003. Marine and Non-Marine Diatoms from the Haida Gwaii Archipelago and Surrounding Coast, Northeastern Pacific, Canada. *In* Bibliotheca Diatomologica, Vol. 48. J. Cramer, Berlin and Stuttgart, Germany.

Pike, J., and Kemp, A.E.S. 1996*a*. Records of seasonal flux in Holocene laminated sediments, Gulf of California. *In* Palaeoclimatology and palaeoceanography from laminated sediments. *Edited by* A.E.S. Kemp. Geological Society, London, Special Publication 116, pp. 157–170.

Pike, J., and Kemp, A.E.S. 1996*b*. Preparation and analysis techniques for studies of laminated sediments. *In* Palaeoclimatology and palaeoceanography from laminated sediments. *Edited by* A.E.S. Kemp. The Geological Society Publishing House, Bath, UK. Special Publication 116, pp. 37–48.

Robinson, S.W., and Thompson, G. 1981. Radiocarbon corrections for marine shell dates with application to southern Pacific northwest coast prehistory. Syesis, **14**: 45–57.

Rogers, G.C. 1988. An assessment of the megathrust earthquake potential of the Cascadia subduction zone. Canadian Journal of Earth Sciences, **25**: 844–852. doi:10.1139/e88-083.

Sancetta, C. 1996. Laminated diatomaceous sediments: controls on formation and strategies for analysis. *In* Palaeoclimatology and Palaeoceanography from Laminated Sediments. *Edited by*

A.E.S. Kemp. Geological Society, London, Special Publication 116, pp. 17–23.

Southon, J.R., Nelson, D.E., and Vogel, J.S. 1990. A record of past ocean-atmosphere radiocarbon differences from the Northeast Pacific. Paleoceanography, **5**: 197–206. doi:10.1029/PA005i002p00197.

Stanford, J.D., Rohling, E.J., Hunter, S.E., Roberts, A.P., Rasmussen, S.O., Bard, E., McManus, J., and Fairbanks, R.G. 2006. Timing of meltwater pulse 1a and climate responses to meltwater injections. Paleoceanography, **21**: 4103–4107. doi:10.1029/2006PA001340.

Stuiver, M., and Braziunas, T.F. 1993. Radiocarbon and ^{14}C ages of marine samples to 10,000 BC. Radiocarbon, **35**: 137–189.

Stuiver, M., and Reimer, P.J. 1986. A computer program for radiocarbon age calibration. Radiocarbon, **28**: 1022–1030.

Stuiver, M., and Reimer, P.J. 1993. Extended ^{14}C database and revised CALIB radiocarbon calibration program. Radiocarbon, **35**: 215–230.

Stuiver, M., Reimer, P.J., Bard, E., Beck, J.W., Burr, G.S., Hughen, K.A., et al. 1998*a*. INTCAL 98 Radiocarbon age calibration 24,000 – 0 cal BP. Radiocarbon, **40**: 1041–1083.

Stuiver, M., Reimer, P.J., and Braziunas, T.F. 1998*b*. High-precision radiocarbon age calibration for terrestrial and marine samples. Radiocarbon, **40**: 1127–1151.

Telford, R.J., Heegaard, E., and Birks, H.J.B. 2004. All age-depth models are wrong: but how badly? Quaternary Science Reviews, **23**: 1–5. doi:10.1016/j.quascirev.2003.11.003.

Thomson, R.E., 1981. Oceanography of the British Columbia Coast. Special Publication of Fisheries and Aquatic Sciences, Vol. 56. The Government of Canada, Ottawa, Ont. 291 p.

Wake, C.P., Dallimore, A., and Fisher, D.A. 2006. North Pacific Climate Workshop Final Report [online]. Available from http://ess.nrcan.gc.ca/extranet/npw/index_e.php [cited February 2008].

Wang, K., He, J., Dragert, H., and James, T.S. 2001. Three-dimensional viscoelastic interseismic deformation model for the Cascadia subduction zone. Earth, Planets, and Space, **53**: 295–306.

Ward, B.C., Wilson, M.C., Nagorsen, D.W., and Driver, J. 2003. Port Eliza Cave: North American West Coast interstadial environment and implications for human migrations. Quaternary Science Reviews, **22**(14): 1383–1388.

Ware, D.M., and Thomson, R.E. 2000. Interannual to multidecadal timescale climate variations in the Northeast Pacific. Journal of Climate, **13**: 3209–3220. doi:10.1175/1520-0442(2000)013<3209:ITMTCV>2.0.CO;2.

Witkowski, A., Lange-Bertalot, H., and Metzeltin, D. 2000. Diatom Flora of Marine Coasts. *In* Iconographia diatomologica, Vol. 7. A.R.G. Gantner, Vaduz, Germany.